Research Article | Vol. 11, No. 2 / 1 February 2020 / Biomedical Optics Express 517
Biomedical Optics EXPRESS

Diffraction-based technology for the monitoring of contraction dynamics in 3D and 2D tissue models

RONAN LE HARZIC,[1,*] INA MEISER,[1] JULIA C. NEUBAUER,[1,2] IRIS RIEMANN,[1] MICHAEL SCHIFFER,[1] FRANK STRACKE,[1] AND HEIKO ZIMMERMANN[1,3,4]

[1] *Fraunhofer Institute for Biomedical Engineering (IBMT), Joseph-von-Fraunhofer-Weg 1, 66280 Sulzbach, Germany*
[2] *Fraunhofer Project Centre for Stem Cell Process Engineering, Neunerplatz 2, 97082 Würzburg, Germany*
[3] *Saarland University, Chair Molecular & Cellular Biotechnology /Nanotechnology, 66123 Saarbrücken, Germany*
[4] *Faculty of Marine Science, Universidad Católica del Norte, Coquimbo, Chile*
[*] *ronan.le.harzic@ibmt.fraunhofer.de*

Abstract: We present a novel optical device developed for the monitoring of dynamic behavior in extended 3D-tissue models in various culture environments based on variations in their speckle patterns. The results presented point out the benefit of the technology in terms of detection, accuracy, sensitivity and a reasonable read-out speed as well as reproducibility for the measurements and monitoring of cardiac contractions. We show that the optical read-out technology is suitable for long time monitoring and for drug screening. The method is discussed and compared to other techniques, in particular calcium imaging. The device is flexible and easily adaptable to 2D and 3D-tissue model screenings using different culture environments. The technology can be parallelized for automated read-out of different multi-well-plate formats.

1. Introduction

Various important fields of work in modern pharmacy and biotechnology use unbiased mass tests of compounds on biological model systems in order to find candidates with favored effects. This so-called screening is a widely applied strategy in drug discovery, toxicology, medical material science and many more areas of life science, where it is difficult to predict promising candidate compounds for specific applications due to a lack of biological understanding or due to the considerable level of bio-system complexity. A typical screening assay consists of a standard procedure, a simplified model of the target organism (or target organ) and an appropriate read-out technology. In order to facilitate mass screenings predominantly two dimensional cell cultures on flat substrates (i.e. monolayers of cells in petri dishes, well plates, lab-on-chips) or suspended single cells are used as models, since such samples are easy to process and analyze [1,2]. Automation of the respective handling and read-out routines is straightforward. However, since most biological processes are not confined to single cells, but have considerable interplay to higher levels of organization, such as tissue, organs, organisms and even populations, cultures of isolated cells are vastly oversimplified models in the majority of cases. This will result in poor correlation of screening results with real-life scenarios [3]. For this reason a paradigm shift is going on in biomedical screening towards the application of higher organized, three dimensional tissue models that reflect native tissue architecture and thus functionality. These models may consist of one or various cell types, if applicable extracellular scaffolds or substrates. Due to the potential of induced pluripotent stem cells tissue models may be prepared disease- and even patient-specific [4]. Such models often require non-conventional, three dimensional culture

#374756 https://doi.org/10.1364/BOE.11.000517
Journal © 2020 Received 5 Aug 2019; revised 31 Oct 2019; accepted 4 Nov 2019; published 2 Jan 2020

Biomedical Optics EXPRESS

environments [5]. A prominent cultivation technique to receive homogeneously sized single- or multicellular aggregates that match physiological appearances is the hanging drop, where cells aggregate in small volumes to 3D constructs due to gravity and the absence of solid interfaces [6,7].

The added value of such sophisticated tissue and organ models is however accompanied by a lack of appropriate read-out technologies. Methods based on absorbance and fluorescence microscopy such as calcium indicators or voltage-sensitive dyes, calcium imaging, surface plasmon resonance reader, patch-clamp technique, multi-electrode arrays (MEAs) and even modern imaging readers [8,9] are not suited as read-out for complex, extended 3D-specimens, in particular using non-conventional culture environments. Cardiac dynamic of 2D-cell cultures were studied using holographic microscopy, revealing its vertical compound. Despite the ability of holography to reveal 3D dynamic, this technology is neither applicable to real 3D tissue with multiple cell layers nor simple enough for parallelization [10–12].

In the extensive field of cardio-vascular drug discovery and drug toxicology as well as embryo toxicity testing usually the collective contractions of cohesive cardiomyocyte cells is recorded as read-out measure [13]. The collective motion formed here is a typical example of biological organization beyond singe cell level. Hence, there is a need for monitoring cardiomyocyte contractions in 3D that has not been covered so far. For 2D-screenings in this field, impedance read-outs by means of MEAs are the state of the art [14–17]. However, as a contact method, it cannot be applied to freely floating 3D cardiac tissue models. Such spatially extended specimens are at present analyzed by visual inspections at the lab microscope. Attempts to automate the read-out using imaging plate readers ended disenchanting due to the size ($\sim$ 0.2-1 mm), non-uniformity and diffusivity of the specimens. Furthermore, dynamics detection requires the acquisition of many image series with very large data set, which would have to be analyzed by complex but robust image analysis routines [18–20]. Overall, there is currently no feasible read-out technology for high-throughput screening of 3D-tissue model dynamics as cardiomyocyte contractions. Against this background, we searched for a sensing technology tailored to the requirements of screenings of dynamic processes within spatially extended specimens. It has to be highly sensitive with respect to the dynamic process, fast enough for high throughput screenings, robust against interferences and minor dislocations of the sample and applicable to various culture environments. Furthermore, it should yield a simple but sophisticated measure of dynamics instead of large data sets from which the dynamics measures have to be extracted by complex analysis. The ultimate goal would be the 96-well-plate parallelization of the technology. To this end, a channel-to-channel pitch of no more than 9 mm distance is required. After assessing a couple of different measuring principles, it turned out that optical diffraction methods met the requirements best. From an instrumental view, our setup resembles a device that was established for microorganism motility studies in 1996 [21]. The method herein quantifies the number of organisms passing the well-confined probing volume per time (focal area times cuvette length) as well as their dwell times within by noise frequency spectroscopy. Unlike the technology presented in this paper, our device illuminates an applicable extent of a solid specimen - preferably all of it - in order to reveal dynamics hidden at specific sites of it instead of illuminating a preferably small volume of a large sample containing independently moving objects. Furthermore, we describe its limits and propose a technical strategy to overcome these.

Herein we report on a tailored optical read-out technology for dynamic behavior in 3D-tissue models based on variations in their speckle patterns (called “Contraction Reader” from here on). We will describe the basic layout of the technology and the specifications of our particular functional model designed as device with a small footprint to allow its integration in standard incubators and cell culture robots. A low susceptibility for interferences and misalignment is in particular important for a later integration into automated screening workflows. It was shown that the technology worked well on different multi-well-plate formats up to 384 wells and with

Biomedical Optics EXPRESS

diverse bottom geometries. The model application will be the important read-out of cardiac contractions in free-floating 3D tissue models [22–24]. Experiments were performed in hanging drop culture, as it is a typical environment for freely floating organoids [25–26].

The Contraction Reader allows the non-contact and marker-free automated optical detection of cardiac contractions in hanging drop / 3D microcarrier as well as 2D monolayer culture by offering a reasonable read-out speed along with high sensitivity and specificity. In practice, the read-out speed was always limited by the biology, i.e. the cardiac beating frequency.

The measurement principle makes use of the interference effects of coherent light diffracted at structure of any size and position in the specimen. Such irregular diffraction patterns are commonly called "Speckle-pattern" [27–29]. It appears in the form of a randomly arranged set of grains on a dark background. Since a structural feature and its movement anywhere in the specimen will influence the whole Speckle pattern. Any dynamic (e.g. cardiac contraction) will alter the entire pattern and hence the amount of light which will be detected and monitored at any site of the pattern. An important feature of the speckle technology is that any illuminated structure in the 3D specimen will contribute to the 2D Speckle pattern. It is therefore possible to assess a 3D sample at once without the need to screen along the optical axis. This drastically speeds up the measurement and keeps the technical implementation simple.

We show that the optical read-out technology is suitable for long time monitoring and for drug screening. The method is discussed and compared to other techniques, in particular calcium imaging

The technologies employed in the Contraction Reader are integrated into a compact body, enabling simple use operations, suitable for drug screenings, in order to evaluate the early pathogenesis of cardiac cells and thereby establish a model that helps to develop and evaluate novel drugs, assay development or cell-based kinetic assays.

2. Materials and methods

2.1. Cell culture

The human induced pluripotent stem cell (hiPSC) line RCi53 (reprogrammed at Censo Biotechnologies Ltd., Midlothian, UK) were cultured under feeder-free conditions on Matrigel (BD, Heidelberg, Germany) in mTeSR medium (Stem cell technologies, Cologne, Germany) according to the maintenance manual of STEMCELL technologies [30]. RCi53s were differentiated into autonomously contracting three dimensional cell aggregates using a customized protocol based on the protocol published by Zhang et al. [31]. In brief, hiPSCs were dissociated using TrypLE (Thermo Fisher Scientific, Schwerte, Germany) to a single cell suspension. 5000 cells were seeded in 40 µl hanging drops using Perfekta 3D hanging drop plates (3D Biomatrix via Sigma-Aldrich, Schwerte, Germany) in the D0 medium as can be seen in Fig. 1A. D0 medium consist of 10 µM Y27632 (Sigma-Aldrich, Darmstadt, Germany), 1x Insulin-Transferrin-Selenium (ITS) (BD, Heidelberg, Germany), 1x Penicillin Streptomycin (PenStrep)/Glutamine (Thermo Fisher Scientific, Schwerte, Germany), 5 ng/ml Fibroblast growth factor 2 (FGF2) (Peprotech, Hamburg, Germany), 2 ng/ml Bone Morphogenetic Protein 4 (BMP4) (R&D Systems, Minneapolis, USA), 1 µM aminopyrimidine derivative CHIR99021 (Axon Medchem, Groningen, The Netherlands) in Knockout Dulbecco's Modified Eagle Medium (DMEM) (Gibco via Thermo Fisher Scientific, Schwerte, Germany). At day 1, 20 µl of the medium was exchanges to TS medium, consisting of 1x transferrin/selenite (TS), 1x lipid additive, 1x PenStrep/Glutamine. 100x TS stock solution was prepared by dissolving 55 mg transferrin (Sigma-Aldrich, Darmstadt, Germany) in 100 ml PBS containing 0.067 mg sodium selenite (Sigma-Aldrich, Darmstadt, Germany). On Day 2, 20 µl per drop was exchanged with the TS medium plus 0.1 µM Wingless/Integrated (WNT) inhibitor (Tocris, Bristol, UK). On day 3, medium exchanges (20 µl) were performed with TS medium plus 0.2 µM WNT inhibitor. From day 4 on, medium exchanges (20 µl) was done with TS medium every 2-3 days. Cell aggregates were kept in hanging drops at all times.

Biomedical Optics EXPRESS

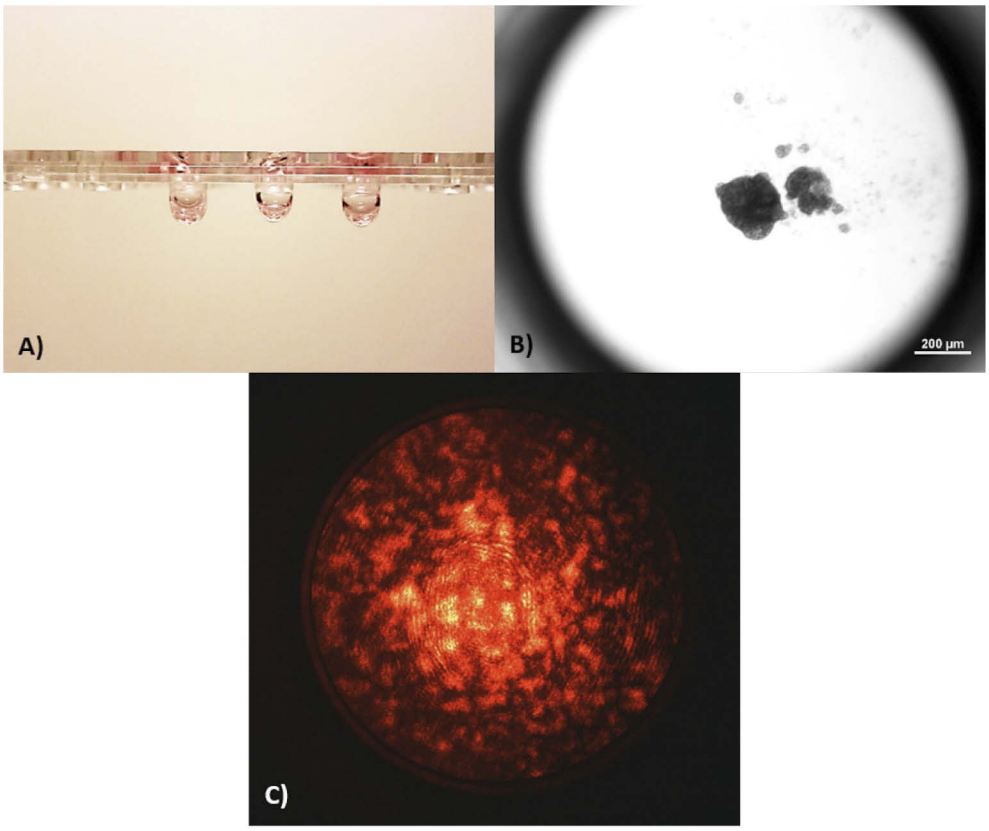

Fig. 1. (A) Side view of hanging drops with a volume of 40 µl in a specific 96 well plate, (B) Microphotography of cardiomyocyte cell aggregates in a hanging drop, (C) Speckle pattern of a cardio cell aggregate.

Using this protocol, first contractions were visible after 6 days. Speckle patterns have been recorded with day 8 cardiac aggregates. A microscopy image of the cardiac cell aggregates and the corresponding Speckle pattern are shown in Fig. 1B and Fig. 1C respectively.

2.2. Contraction reader functional model

A photographic and a schematic overview of the Contraction Reader device is shown respectively in Fig. 2(A) and 2(B). The emission module is composed of a 5.6 mm compact and inexpensive AlGaInP continuous wave (CW) laser diode emitting in the visible at a wavelength of 635 nm and delivering up to 30 mW of maximum power. The intensity and size of the slightly divergent laser beam is controlled by a motorized iris diaphragm with 7 mm maximal aperture.

The laser beam maximal intensity at the output of the emission module is 10 mW at maximal aperture. A 0.15 numerical aperture (NA), 18.4 mm short focal length aspheric lens is used to focus the laser beam to a spot size of 6-8 µm into the cardiac body in the hanging drop which can be up to several hundred µm in size (of about 200 µm in the example shown in the Fig. 1(B)). Such lens allows the generation of relatively large speckle grains and reduces aberrations of the elliptical divergent laser beam. Thus, a specimen that large is not illuminated entirely in this particular configuration. However, we found spatially confined contracting sites outside the probing volume to be detectable in freely floating organoids. Nevertheless, in order to extend the illuminated probing volume, the illumination can be tuned out of focus. This leads to a finer

Biomedical Optics EXPRESS

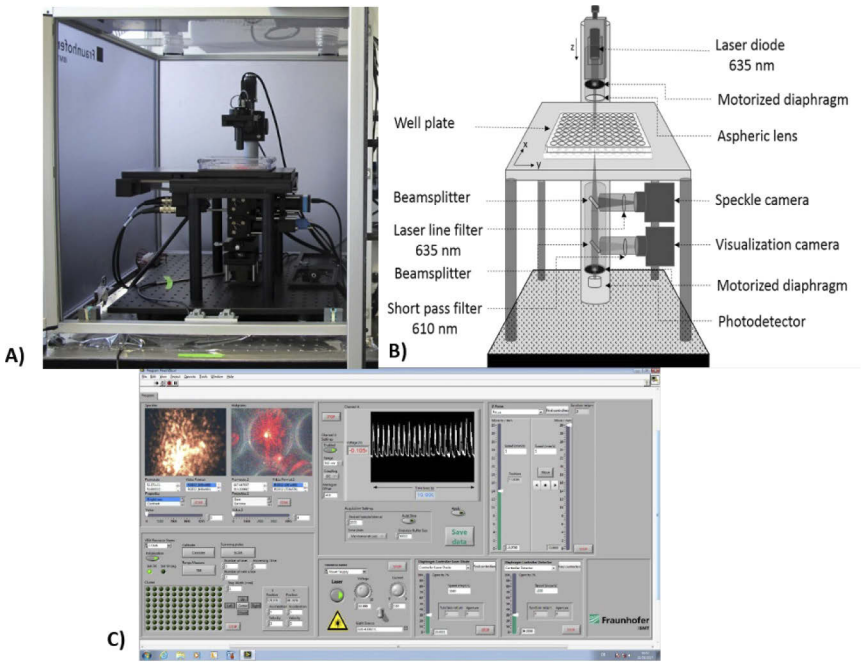

Fig. 2. Contraction Reader device photography in its safety enclosure (A), schematic overview of the different elements constituting the optical device (B), Intuitive user interface for control, visualization and signal monitoring (C).

grained Speckle pattern, which still contains the information about specimen dynamics. The emission module is mounted on a motorized linear stage to allow an accurate adjustment of the focus of the laser beam in z for the control of an optimal speckle pattern and the corresponding amount of light to be detected and monitored. Furthermore, manual mini translation stages allows the adjustment in x and y.

The 96 hanging drops well plate is placed on a x, y motorized stage with a travel range of 120×80 mm, a repeatability < 1 µm, an accuracy of +/- 3 µm, a resolution of 0.01 µm. In parallel, a 2-axes joystick allows rapid stage movement across the complete travel range while also accurately positioning within microns.

For long term stable measurements and monitoring conditions, it is possible to integrate a stage top incubator for multi-well plates in the centerpiece of the x, y motorized stage that fit K-Frame Inserts, consisting of a heated plate with a heated glass bottom, and also a heated lid that is designed to keep cells at 37°C and therefore prevent condensation effects in multi-well plates. The glass top of the lid, the glass bottom of the plate and the plate itself are actively heat controlled.

The detection unit includes three modules, 2 cameras for the visualization and control and a photodetector for the monitoring of the signal as can be seen in the scheme (Fig. 2B). In the first stage, the generated speckle pattern evoked above is reflected by a beamsplitter, filtered by a 635 ± 2 nm laser line filter and projected to a CMOS USB color camera (pixel size: 3.75 µm x 3.75 µm, resolution: 1280×960 pixels, frame rate: up to 60 fps), for the visualization and monitoring of the fluctuations related to the cardiac contractions.

In the second stage, a second CMOS USB color camera (pixel size: 2.2 µm x 2.2 µm, resolution: 2592×1944 pixels, frame rate: up to 6 fps), allows the visualization of the wells position and laser beam adjustment. The bottom of the well plate is illuminated by the use of a variable fiber

Biomedical Optics EXPRESS

cold light source, which is reflected by a beamsplitter to the camera passing before throw a 610 nm cut off short-pass filter.

The actual dynamic read-out is conducted at the third stage. The Speckle pattern evoked by the tissue model's internal structures is directed onto the front of a high sensitive amplified Si switchable gain photodetector. Already a contraction dynamic in a minute part of the tissue model leads to a significant alteration of the Speckle pattern on the screen while the overall intensity of the pattern is approximately constant. Hence recording the intensity of the whole pattern will hide the dynamic. To this end, the detector is mounted on an accurate x, y translation stage for positioning optimization and as for the emission module, a motorized iris diaphragm cuts out a certain fraction of the pattern that is transmitted to the detector. The signal becomes maximum when the diaphragm aperture is on the scale of the speckle grains. A very beneficial feature of Speckle patterns is that dynamics in a particular site of the illuminated volume lead to variations of the entire pattern. Therefore, the position of the diaphragm aperture cannot be principally wrong. A dislocation between aperture and pattern will alter the amplitude and the shape of the contraction spikes, but not their repetition frequency. Even negative contraction spikes occur. The contraction reader has been conceived to allow the measurement of cardiac cells with very low contraction signals quasi imperceptible to the eye and with relative good signal to noise ratio (SNR) which is defined as the ratio of signal power to the noise power ($SNR_{dB} = 10log\ [(A_{Signal}/A_{Noise})^2]$). To optimize signal detection recording, the amplified photodetector can detect very weak signals by adjusting an eight- position rotary switch, which allows the user to vary the gain in 10 decibel (dB) steps.

The software provides an easy to use interface as depicted in Fig. 2C. It allows the control of the laser diode. It displays as explained above simultaneously in live the speckle pattern and the bottom of the well plate with the visualization of up to 9 wells. The user can select the frame rate and the video format as well as parameters such as brightness, contrast... The signal detected is displayed on a waveform graph. Parameters such as time and voltage sensibility can be modified, the signal can be recorded for short to long time measurements. The signal data can be saved as a text file and exported in data analysis and graphics programs. The stage can directly be shifted on the desired well by simply clicking on the mouse on the scheme representing the 96 wells. Some sequences can also be programmed for an automatic positioning on a defined number of wells, set up velocity and delay for each axis. The user controls the focus and the two iris diaphragms as discussed above by the different gauges as shown on the left of the interface view. The contraction frequency was calculated as the total time between the first and the last peak of a complete or part of a curve divided by the number of peaks as well as its absolute error, which is the difference between the mean value and the maximal and minimal value

The contraction reader is mounted on a vibration isolated platform, the complete unit dimensions are $450 \times 450 \times 450$ mm for a weight of 15 kg. Against eventual laser exposure, the Contraction Reader is placed in a safety enclosure ($600 \times 600 \times 600$ mm) as can be noticed in Fig. 2A.

3. Results and discussion

A section of the contraction signal of a cardio cell cluster cultivated as explained above is depicted in Fig. 3.

The average contraction frequencyis about 3.9 ± 0.8 s. One can observe amplitude differences from peak to peak due to the inherent motions of the specimen in the hanging drop. The period between the contraction of peak 1 and peak 2 is 4.7 s. The period between peak 7 and 8 is 3.5 s. The signal to noise ratio (SNR) is about 20 dB. The relative amplitude as well as the SNR are functions of the contraction strength of the cardio cell cluster. As already mentioned, the best signals and SNR are obtained by cutting out an area of the speckle pattern in the order of the Speckle grains by adjusting the diaphragm aperture accordingly. The size of these latters depends on the focus position of the emission module accurately adjusted by the motorized linear

Biomedical Optics EXPRESS

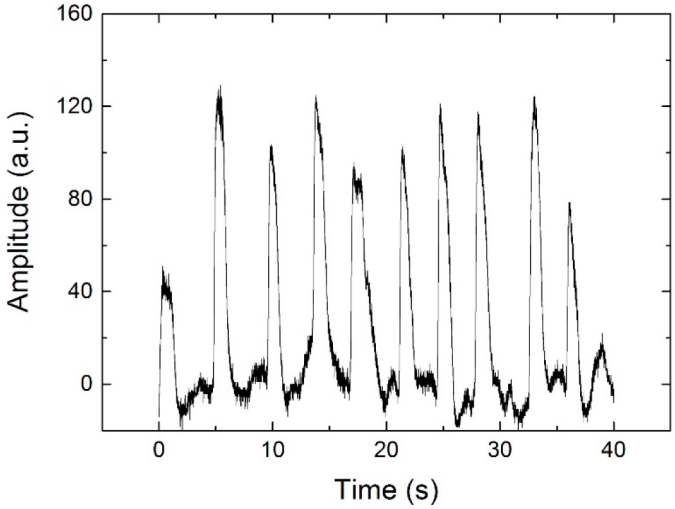

Fig. 3. Monitored signal of the speckle pattern depicted in Fig. 1(C). The period of the contractions is of 3.9 ± 0.8s with an SNR of about 20 dB.

stage. Figure 4 shows three patterns taken at −1 mm (Fig. 4A), + 1 mm (Fig. 4C) on either side of the optimal focus positon (Fig. 4B) where the speckle pattern has the biggest grain sizes.

By adjusting the aperture of the both motorized iris diaphragms, the signal can be accurately and slightly optimized by controlling the size of the laser beam and its intensity in the emission module and speckle grain filtering as well as the amount of light to be detected in the detection module. This optimization operation is quite easy, and intuitive to obtain a good signal with high SNR relatively rapidly. Once this procedure is finished, it is very simple to recover directly good signals when shifting the stage on the desired other wells of the 96 wells plate if the cardiac aggregate is found to be centered at the bottom of the drop as expected. Minor adjustments of the relative lateral positions of illumination beam, specimen and detection aperture usually help to optimize the signal strength and shape. Since the specimens are freely floating (and rotating) in the medium drop, the optimal beam and aperture positions are not necessarily conserved during a measurement. These specimen motions are the origin of the significant amplitude and shape variations of the contractions spikes during a measurement (see Fig. 3 and Fig. 5). Hence amplitude is not a meaningful measure in this setup. Yet contraction frequency determination is unaffected by specimen motions. We propose and simulate a technical advancement to overcome these limitations and to make amplitude and shape of the contraction signals meaningful a little further down in this paragraph.

The recording and signal monitoring of the contractions in a well is carried out in real time without any image analysis algorithms. The temporal resolution of the technology is only limited by the maximum read-out speed of the photodetector and oscilloscope (here, ~ 100 ns). The practical time it takes to determine the contraction frequency is given by biology. The minimum time is the period of the contraction, i.e. the time between two contractions. In general, the researcher likes to have more statistical relevance. Therefore, a specimen will be investigated for more than just two beatings. Also the maximum beating frequency seems to be limited by biology: while the frequency increases, the duration of a contraction remains constant. Hence, the maximum beating rate is limited by the contraction lapse time. A long beating trace of a cell aggregate obtained from another iPSC line using the same differentiation protocol has been recorded and results are depicted in Fig. 5.

Biomedical Optics EXPRESS

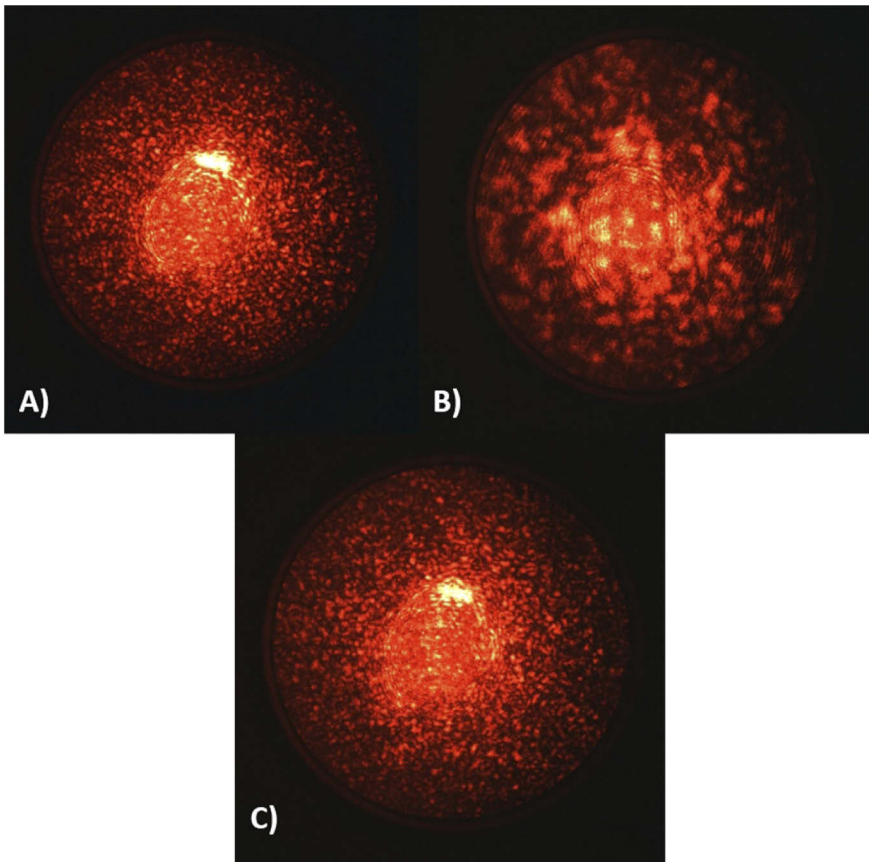

Fig. 4. Speckle patterns recorded at (A) −1 mm, (B) 0 mm (see **Visualization 1**), (C) +1 mm defocusing. The Speckle grain size decreases significantly compared to sample-in-focus conditions. Large grains lead to strong signals. However, if defocused detection is necessary, e.g. for wider illumination areas, the signal can still be extracted from the finer patterns

Contractions have been recorded for 10 minutes as depicted in Fig. 5(A). A multitude of detected peaks can be observed here. To distinguish and analyze the peaks, three parts of the monitoring have been zoomed, at the beginning, from 0 to 60 s (Fig. 5(B)), at the middle, from 300 to 360 s (Fig. 5(C)), and at the end, from 540 to 600 s (Fig. 5(D)). At first sight, the peaks are amply distinguishable and seem to be regular. Average beating periods have been measured for the three different parts. The contractions period, as can be seen in Fig. 5(E) remains basically constant at about 2.35 ± 0.05 s. Measurements with good signal detection and reproducibility can be performed on long time series with good stability and very few fluctuations if the temperature is maintained at ± 37°C. A non-constant temperature leads to considerable alterations of the contraction frequency. After a certain time at ambient temperature cardiac contraction even stopped. Therefore, temperature control is important in the case of long-term measurements when adding compounds for drug screening for example to study the effect and impact on contraction period as well as amplitude variation. Again, specimen motions may have played a role in the variations of amplitude and shape here. The technical strategy to overcome these limitations due to specimen motions is about using multiple detection apertures (or detector pixels). Summing or averaging the readings of these "pixels" would lead to a constant, noisy background without contraction spikes, since they average out each other. Hence, each pixel reading is processed first

Biomedical Optics EXPRESS

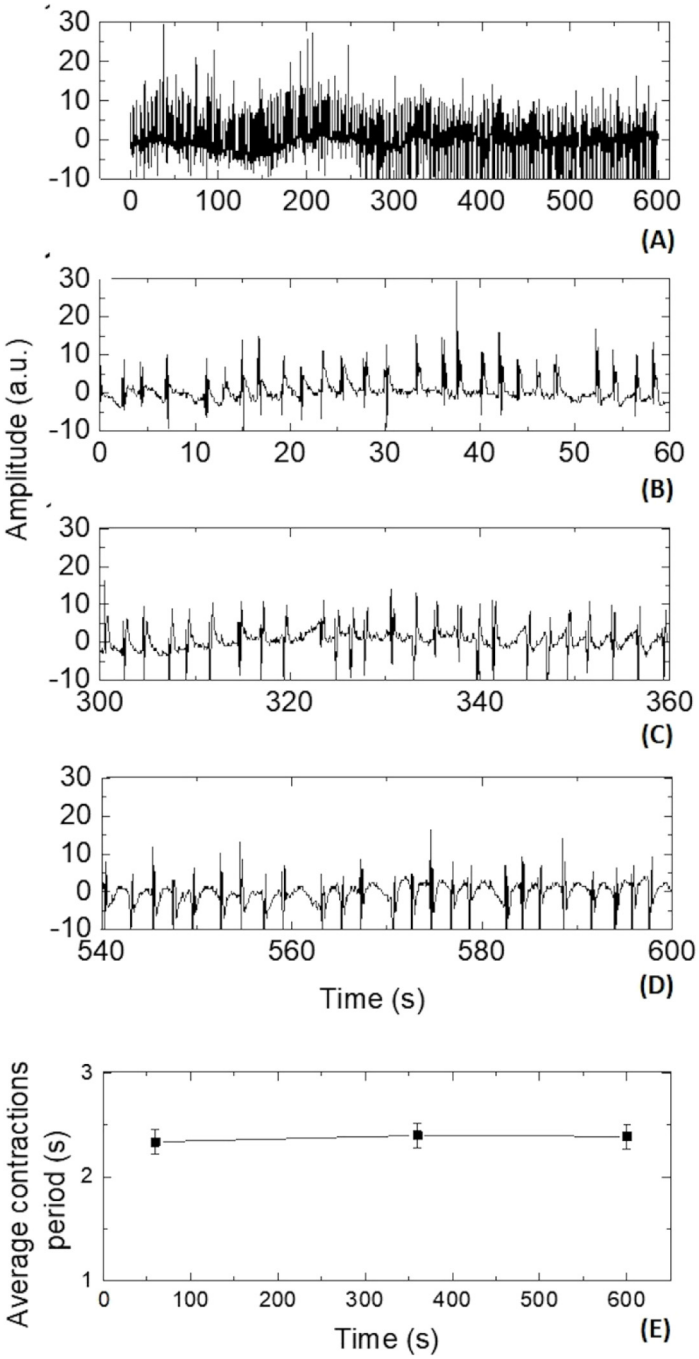

Fig. 5. 10 min time monitoring of the contractions of cell aggregates in hanging drop (A). Zoom of the contractions signal from 0 to 60 s (B), from 300 to 360 s (C), and from 540 to 600 s (D). Average frequencies measured at 60, 360 and 600 s (E). The contractions period stays almost constant at 2.35 ± 0.05 s. Note the variations in amplitude and shape. The contraction spikes are partially negative.

Biomedical Optics EXPRESS

and then summed up. The processing consists of a differentiation step to separate the dynamic part from any background and a subsequent rectifying step (e.g. modulus or square). The results of the processing are ultimately summed up to yield a simple measure of contraction dynamic, that is found to be widely reproducible and insensitive to specimen motions as long as the major fraction of the speckle pattern is investigated. To our knowledge, such a detector array with built-in data processing is not commercially available. So, we used the recorded videos of Speckle patterns from the Speckle camera, subdivided it in 192 regions of interest (ROIs) and processed the integrated intensity data of each ROI afterwards as described using Nikon microscopy software. The resulting contraction traces simulates the proposed detector data and

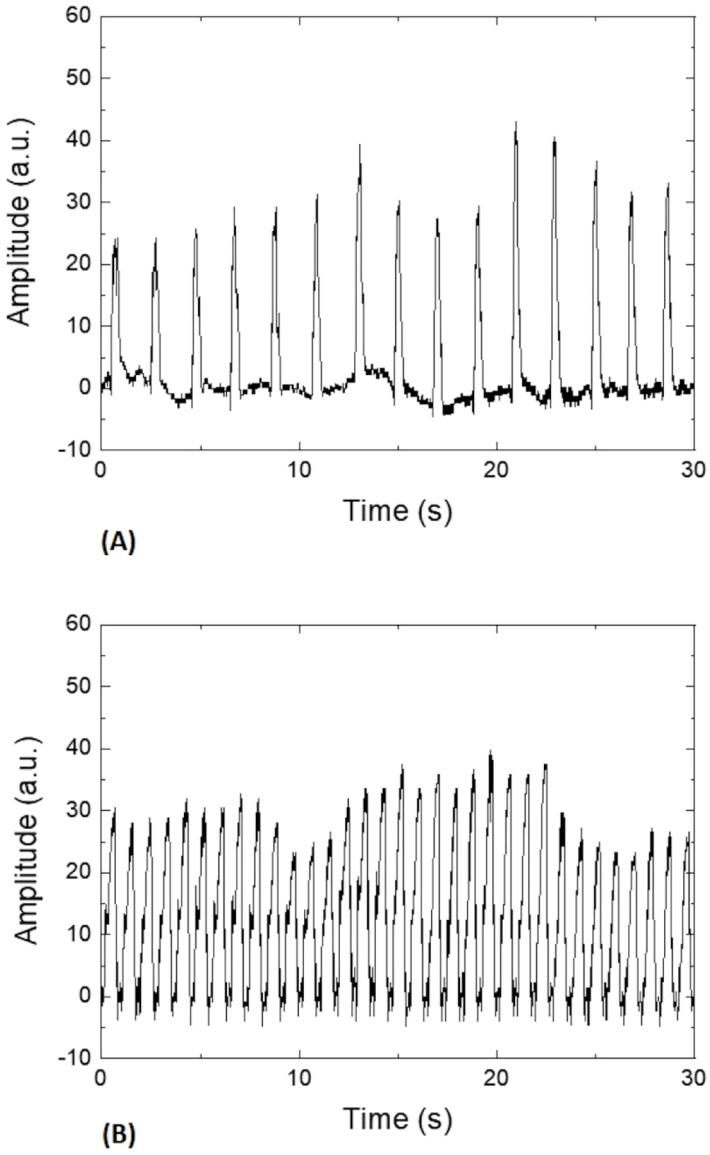

Fig. 6. Addition of Isoprenalin, a stimulant compound. Contractions were measured without addition (A), the period of the contractions is 2 ± 0.05 s and with addition (B), the period is reduced to 0.9 ± 0.05 s, the beating rhythm is faster.

Biomedical Optics EXPRESS

are found to be very consistent in amplitude and shape. As well, the contraction trace shape clearly shows segments that may be associated to contraction and relaxation of the cardiac cycle. We used this simulated technology in the investigation on applicability of different plate formats as well as on the correlation to calcium spikes (see Fig. 8 and Fig. 9).

To evaluate the pertinence of the Contraction Reader technology for drug screening applications and studies, an experiment has been performed by adding a stimulant compound: Isoprenalin. This latter is a synthetic derivative of adrenaline, used mainly as bronchodilator and heart stimulant for the treatment of bradycardia (slow heart rate), heart block, and rarely for asthma. For this purpose, a 10 µM Isoprenalin solution has been prepared. 4 µl of the initial hanging drop medium volume of 40 µl were removed and instead 4 µl of Isoprenalin were injected in the drop. Thus, the total volume remains the same, 40 µl and the concentration of Isoprenalin in the complete drop is of 1 µM. Recordings of the contractions were performed first without the addition of Isoprenalin and second after addition of the Isoprenalin until a few minutes that the solution mixes homogeneously and penetrates into the aggregate. Results are shown in Fig. 6(A) and 6(B) respectively.

As can be observed, the frequency of contractions significantly increased after the addition of Isoprenalin. Starting with an average period of 2 ± 0.05 s, the addition accelerates the contraction to an average period of $0{,}9 \pm 0.05$ s. The amplitudes and the related alterations cannot be used due to the inherent fluctuations from the freely floating specimen. The results shown here are convincing and indicate that the Contraction Reader is suitable for drug screening.

Thanks to the potential of the Contraction Reader to monitor an extended 3D volume at once, it is possible to detect and distinguish two unrelated frequencies of cardiac tissue models, arising from separated contracting sites in the same specimen as presented in the Fig. 7. There is no addition of stimulant compound as Isoprenalin in this example. It is possible to measure the contraction frequencies of two different beating centers in the same cardiac cell aggregate at the same time.

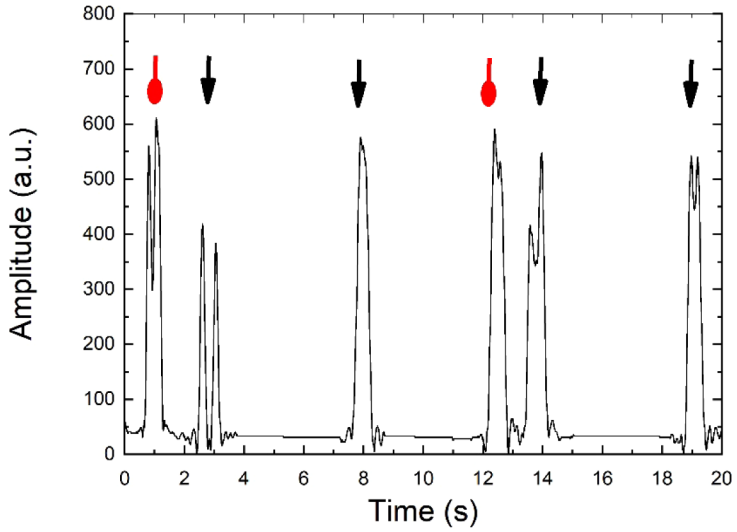

Fig. 7. Data showing an overlay of two independent contraction traces (see arrows) with two independent frequencies. This is due to two separated contracting sites within the same cardiac tissue model.

In order to evaluate the versatility and flexibility of the Contraction Reader device, comparison measurements have been performed on several plate formats and geometries. For this purpose, recording of speckle patterns and contraction signals of the same cardio cells cluster has been

Biomedical Optics EXPRESS

performed using the described simulation technique of a detector array. The same aggregate was transferred first in a 96 hanging drop well plate, then in a 384 hanging drop well plate, following with a 96-V-bottom well plate, then in a 96-U-bottom well plate and finally in a LabBag (innovative safety and inexpensive mini-lab in the form of a plastic bag for a closed, surface-based cultivation of stem cells [32]. The results are depicted in Fig. 8. As can be observed, speckle patterns and contraction signals were generated in all cell culture devices. Furthermore, the contraction signals are in all cases detectable, recordable and comparable in quality, intensity and sensitivity. The Contraction Reader is easily adaptable to 2D and 3D-tissue model screenings using different culture environments.

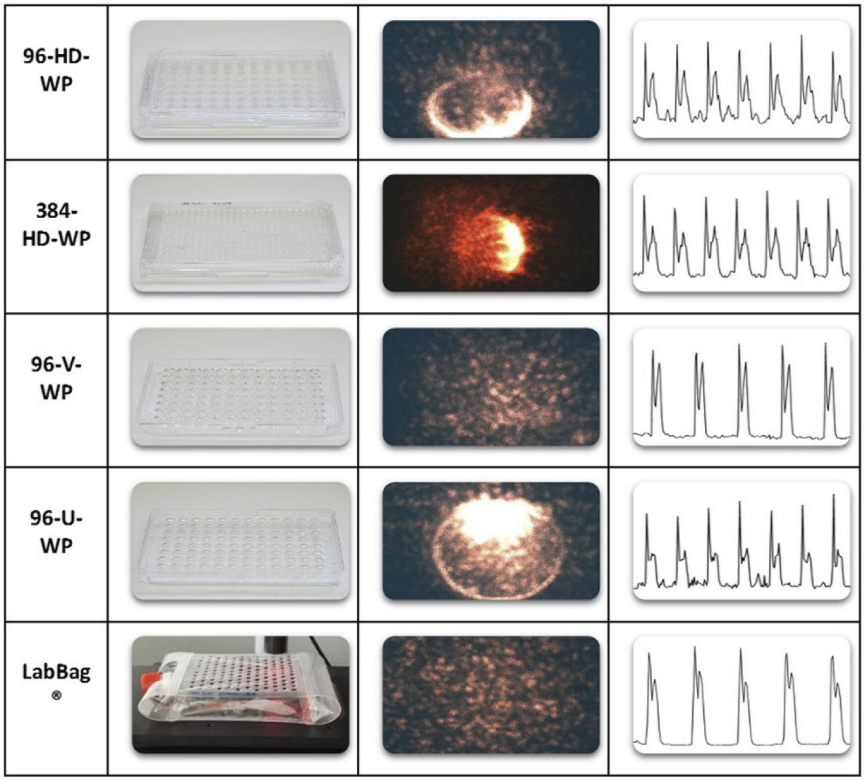

Fig. 8. Comparison measurements of contractions on several plate formats and geometries in 2D and 3D tissue models. In a 96 and 384 hanging drop well plate, in a 96-V and -U bottom well plate and in a LabBag.

Hereafter a comparison of the Contraction Reader with the calcium imaging technique has been performed using commercial cardiomyocytes, Cor.4U (Axiogenesis, Cologne, Germany) in addition to the hiPSC cell linies used in all the experiments presented in this paper so far. For visualization of fluorescent images, the fluorescent dye fluo-4-AM (Thermo Fisher Scientific, Schwerte, Germany) has been used as calcium indicator. 50 µg of Fluo-4-AM were dissolved in 50 µl of DMSO with 20% Pluronic F127 (Sigma-Aldrich, Darmstadt, Germany). Caution is advised not expose the dye solution too much to the light. To obtain a 10 µM solution, 50 µl of the mixture were mixed with 4.508 ml of appropriate cell culture medium. Subsequently, a 96-well microtiter plate with spheroids was taken from the incubator and 80 µl of the medium were removed with a multichannel pipette. Next, 80 µl of the medium with dye were added to the cells and the multiwell plate is incubated for one hour in the incubator at 37 °C and 5% CO_2. After the lapse of time, 80 µl of the medium were removed again and the specimen were

Biomedical Optics EXPRESS

washed twice with fresh medium without dye. Then the microtiter plate was incubated again for 20 minutes at 37 ° C and 5% CO_2. At least, 1 µM of Isoprenalin was added in the spheroids to compare both systems in the conditions of drug screening.

The fluorescence images were taken on a SMZ25 stereomicroscope (Nikon, Tokyo, Japan). The sample was illuminated from below with a fluorescent lamp with the excitation spectrum of the dye (494 nm). The dye emits light at a wavelength of 506 nm. The videos were recorded with a camera. The contraction rate of Cor.4U spheroids was determined from the calcium signals. The microtiter plate was then immediately transferred afterwards to the Contraction Reader and the speckle patterns and contractions recorded. Both units use a heating chamber to control the temperature of the spheroids. A 30 s signal has been recorded several times in both case. Figure 9 shows the direct comparison of the fluorescence measurement and the speckle dynamics. Speckle dynamics have been again recorded by the simulated detector array technique.

The peaks of the Contraction Reader show distinctly separate movements. The calcium measurement shows the rapid influx of Ca^{2+} associated with fluorescence and the subsequent relaxation of the signal. The average contraction rate is of $1{,}19 \pm 0{,}05$ s and $1{,}17 \pm 0{,}05$ s for the calcium imaging and for the Contraction Reader respectively. The measurements are quasi similar.

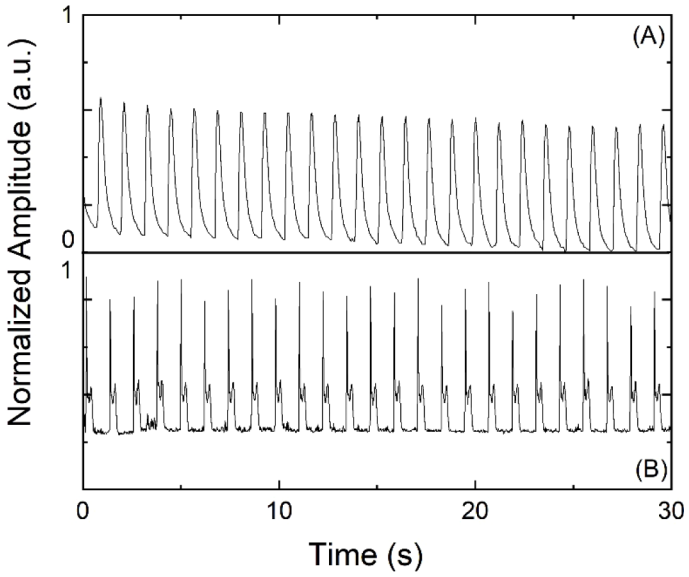

Fig. 9. Comparison of the contraction signal measured by Calcium Imaging (A) and by the Contraction Reader (B). Both traces were recorded on the same specimen, but not simultaneouisly.

As already mentioned, there are a number of methods of analysis for toxicological effects. These differ however strongly in their application. MEAs and the patch clamp technique are not suitable for 3D cultures and provide only electrophysiological data. They are therefore difficult to compare with the Contraction Reader. Better comparable techniques are video microscopy and calcium imaging. Both techniques use a video recording. However, microscopes have the disadvantage that the optics are very complex and thus difficult to parallelize. In addition, a correct focus of the sample is very important. In comparison, the technique of the Contraction Reader is very simple, accurate focusing of the sample is not important. Video microscopy has advantages only in the measurement of cells and the determination of motion vectors. Calcium Imaging is a widely used and established technique for visualizing free Ca^{2+} in cells. Since

Biomedical Optics EXPRESS

Ca^{2+} is involved as a messenger in many cellular processes, the technique can also be used in many ways. Among other things, calcium plays an important role in the contraction of cardiomyocytes [33]. Calcium imaging is probably the most widely used technique for the study of cardio-toxicological effects. A large number of cardio-toxicological substances have already been tested with the existing automated systems [34]. Although this technique is preferred for 2D cultures, but 3D spheroids can also be analyzed. Calcium imaging uses a fluorescent dye that can bind to free calcium in the cells and make calcium currents visible in fluorescence contractions [35].

With the Contraction Reader, no information about ion currents can be measured, but it shows the dynamics of movement. As shown in Fig. 9, the peaks show the contraction (first peak), the relaxation (second peak) and the duration of the complete movement. The calcium signal contains no direct information about the actual movement. Since the calcium influx is directly coupled with the contraction, the contraction rate can be determined by the calcium peaks. However, there are diseases and substances that decouple calcium flow from mechanical movement (Huebsch et al., 2015). A parallel measurement of the two techniques would be very interesting. This would allow the movement phases to be directly linked to the calcium signal. A comparable experiment in 2D was already done using standard video microscopy and calcium imaging [35]. Even with the Contraction Reader such comparisons would be possible. The Fluo-4-AM dye used should remain largely unaffected by the measurement on the Contraction Reader. The excitation wavelength of Fluo-4 (494 nm) does not coincide with the wavelength of the laser (635 nm) used in the Contraction Reader. Since the effects of many substances in 2D and to a lesser extent in 3D cultures were investigated with calcium imaging [34], supplementing calcium signals with movement patterns would be very interesting.

In direct comparison, calcium imaging has the advantage of collecting information on calcium influx. However, this advantage also includes some disadvantages. By using a dye, the application is highly invasive and due to the stability of the dye also not suitable for long-term experiments. In addition, as already mentioned, no information is provided about the actual movement of the contraction. Furthermore, the measurement in the Contraction Reader is much easier to perform and requires no preparation time or expensive dyes.

4. Conclusion

In summary, we presented a novel optical device developed for the monitoring of dynamic behavior in 3D-tissue models based on variations in their Speckle patterns. The results presented point out the benefit of the technology in term of detection, accuracy, sensitivity and a reasonable read-out speed as well as reproducibility of the measurements and recordings regarding periods and amplitudes of cardiac contractions in time.

In principle, it would be possible to operate many channels in parallel in order to speed up the screening of multiwell-plates by illuminating every well by multiplying the number of mini laser diodes or using a fiber bundle technology as well as multi mini detectors or a complete special sensor to improve the detection in term of stability and accuracy. Each signal could be monitored in parallel. For many semi-automated screening workflows using tissue models or organoids and a dynamic read-out, such a technology could close the automation gap.

As demonstrated in the different results as well as compared to calcium imaging, the Contraction Reader is suitable for long time monitoring and for drug screening setups, which are of major interest for the pharmaceutical industry as well as for all forms of cardiac studies and researches. The Contraction Reader could be easily integrate in all sort of cell culture robots for the automated cultivation of cells as for example a TECAN Evo200 platform (Tecan, Männedorf, Switzerland), or a CompacTSelecT system (TAP/Satorius, Royston, UK).

We have shown that the Contraction Reader is also easily adaptable to 2D and 3D-tissue models screenings using different culture environments and cell culture multiwell plates.

Biomedical Optics EXPRESS

Furthermore, our studies indicate that the Contraction Reader could be suitable for all forms of researches on transparent organisms regarding the detection of the heart beating in drosophila animals as well as of various types of rhythmic movements such as respiration, chewing and locomotion for their survival.

Funding

European Community's Seventh Framework Programme (HEALTH-F5-2013-601865 "DropTech").

Disclosures

The authors declare that there are no conflicts of interest related to this article.

References

1. Y. Zhou, S. Zhu, C. Cai, P. Yuan, C. Li, Y. Huang, and W. Wei, "High-throughput screening of a CRISPR/Cas9 library for functional genomics in human cells," Nature **509**(7501), 487–491 (2014).
2. V. Planelles, F. Wolschendorf, and O. Kutsch, "Facts and Fiction: Cellular Models for High Throughput Screening for HIV-1 Reactivating," Curr. HIV Res. **9**(8), 568–578 (2011).
3. A. Abbott, "Cell culture: biology's new dimension," Nature **424**(6951), 870–872 (2003).
4. J. T. Dimos, I. Griswold-Prenner, M. Grskovic, S. Irion, C. Johnson, and E. Vaisberg, "Induced Pluripotent Stem Cells as Human Disease Models," Annu. Rep. Med. Chem. **46**, 369–383 (2011).
5. F. Pampaloni, E. G. Reynaud, and E. H. Stelzer, "The third dimension bridges the gap between cell culture and live tissue," Nat. Rev. Mol. Cell Biol. **8**(10), 839–845 (2007).
6. M. Drewitz, M. Helbling, N. Fried, M. Bieri, W. Moritz, J. Lichtenberg, and J. M. Kelm, "Towards automated production and drug sensitivity testing using scaffold-free spherical tumor microtissues," Biotechnol. J. **6**(12), 1488–1496 (2011).
7. M. Chen, Y. Q. Lin, S. L. Xie, H. F. Wu, and J. F. Wang, "Enrichment of cardiac differentiation of mouse embryonic stem cells by optimizing the hanging drop method," Biotechnol. Lett. **33**(4), 853–858 (2011).
8. C. W. Scott, M. F. Peters, and Y. P. Dragan, "Human induced pluripotent stem cells and their use in drug discovery for toxicity testing," Toxicol. Lett. **219**(1), 49–58 (2013).
9. E. Laurila, A. Ahola, J. Hyttinen, and K. Aalto-Setälä, "Methods for in vitro functional analysis of iPSC derived cardiomyocytes - Special focus on analyzing the mechanical beating behavior," Biochim. Biophys. Acta, Mol. Cell Res. **1863**(7), 1864–1872 (2016).
10. B. Rappaz, I. Moon, F. Yi, B. Javidi, P. Marquet, and G. Turcatti, "Automated multi-parameter measurement of cardiomyocytes dynamics with digital holographic microscopy," Opt. Express **23**(10), 13333–13347 (2015).
11. N. Shaked, L. Satterwhite, N. Bursac, and A. Wax, "Whole-cell-analysis of live cardiomyocytes using wide-field interferometric phase microscopy," Biomed. Opt. Express **1**(2), 706–719 (2010).
12. I. Moon, K. Jaferzadeh, E. Ahmadzadeh, and B. Javidi, "Automated quantitative analysis of multiple cardiomyocytes at the single-cell level with three-dimensional holographic imaging informatics," J. Biophotonics **11**(12), e201800116 (2018).
13. A. E. M. Seiler and H. Spielmann, "The validated embryonic stem cell test to predict embryotoxicity in vitro," Nat. Protoc. **6**(7), 961–978 (2011).
14. Y. A. Abassi, B. Xi, N. Li, W. Ouyang, A. Seiler, M. Watzele, R. Kettenhofen, H. Bohlen, A. Ehlich, E. Kolossov, X. Wang, and X. Xu, "Dynamic monitoring of beating periodicity of stem cell-derived cardiomyocytes as a predictive tool for preclinical safety assessment," Br. J. Pharmacol. **165**(5), 1424–1441 (2012).
15. M. K. B. Jonsson, Q.-D. Wang, and B. Becker, "Impedance-based detection of beating rhythm and proarrhythmic effects of compounds on stem cell-derived cardiomyocytes," Assay Drug Dev. Technol. **9**(6), 589–599 (2011).
16. S. D. Lamore, C. W. Scott, and M. F. Peters, "Cardiomyocyte Impedance Assays-Assay Guidance Manual", in Assay Guid. Man. (2015). (http://www.ncbi.nlm.nih.gov/pubmed/25855850).
17. M. F. Peters, C. W. Scott, R. Ochalski, and Y. P. Dragan, "Evaluation of Cellular Impedance Measures of Cardiomyocyte Cultures for Drug Screening Applications," Assay Drug Dev. Technol. **10**(6), 525–532 (2012).
18. A. Kamgoué, J. Ohayon, Y. Usson, L. Riou, and P. Tracqui, "Quantification of cardiomyocyte contraction based on image correlation analysis," Cytometry, Part A **75A**(4), 298–308 (2009).
19. A. Ahola, A. L. Kiviaho, K. Larsson, M. Honkanen, K. Aalto-Setälä, and J. Hyttinen, "Video image-based analysis of single human induced pluripotent stem cell derived cardiomyocyte beating dynamics using digital image correlation," BioMed. Eng. Online **13**(1), 39 (2014).
20. T. Hayakawa, T. Kunihiro, T. Ando, S. Kobayashi, E. Matsui, H. Yada, Y. Kanda, J. Kurokawa, and T. and Furukawa, "Image-based evaluation of contraction - relaxation kinetics of human-induced pluripotent stem cell-derived cardiomyocytes: Correlation and complementarity with extracellular electrophysiology," J. Mol. Cell. Cardiol. **77**, 178–191 (2014).
21. J. A. Cole and M. H. Tinker, "Laser speckle spectroscopy - a new method for using small swimming organisms as biomonitors," Bioimaging **4**(4), 243–253 (1996).

Biomedical Optics EXPRESS

22. C. L. Mummery, "Perspectives on the Use of Human Induced Pluripotent Stem Cell-Derived Cardiomyocytes in Biomedical Research," Stem Cell Rep. **11**(6), 1306–1311 (2018).
23. M. Devarasetty, S. Forsythe, T. D. Shupe, S. Soker, C. E. Bishop, A. Atala, and A. Skardal, "Optical Tracking and Digital Quantification of Beating Behavior in Bioengineered Human Cardiac Organoids," Biosensors **7**(4), 24 (2017).
24. M. Devarasetty, A. R. Mazzochi, and A. Skarda, "Applications of Bioengineered 3D Tissue and Tumor Organoids," BioDrugs **32**(1), 53–68 (2018).
25. B. Nugraha, M. F. Buono, L. von Boehmer, S. P. Hoerstrup, and M. Y. Emmert, "Human Cardiac Organoids for Disease Modeling"," Clin. Pharmacol. Ther. **105**(1), 79–85 (2019).
26. C. Zuppinger, "3D Cardiac Cell Culture: A Critical Review of Current Technologies and Applications," Front. Cardiovasc. Med. **6**, 87 (2019).
27. J. C. Dainty, *Laser Speckle and Related Phenomena*, 2nd ed. (Springer-Verlag, 1989).
28. K. Basak, M. Manjunatha, and P. K. Dutta, "Review of laser speckle-based analysis in medical imaging," Med. Biol. Eng. Comput. **50**(6), 547–558 (2012).
29. D. Briers, D. D. Duncan, E. Hirst, S. J. Kirkpatrick, M. Larsson, W. Steenbergen, T. Stromberg, and O. B. Thompson, "Laser speckle contrast imaging: theoretical and practical limitations," J. Biomed. Opt. **18**(6), 066018 (2013).
30. Manual Stem cell technologies: "Maintenance of human induced pluripotent stem cells" www.stemcells.com, 27.12.2016.
31. M. Zhang, J. S. Schulte, A. Heinick, I. Piccini, J. Rao, R. Quaranta, D. Zeuschner, D. Malan, K. P. Kim, A. Röpke, P. Sasse, M. Araúzo-Bravo, G. Seebohm, H. Schöler, L. Fabritz, P. Kirchhof, F. U. Müller, and B. Greber, "Universal cardiac induction of human pluripotent stem cells in two and three-dimensional formats: implications for in vitro maturation," Stem Cells **33**(5), 1456–1469 (2015).
32. M. Gepp, R. Duckstein, F. Kayatz, N. Rodler, Z. Scheuerer, J. C. Neubauer, K. Lachmann, C. Stramm, A. Liebmann, M. Thomas, and H. Zimmermann, "Labbag - a versatile bag-based cultivation system for expansion, differentiation and cryopreservation of human stem cells," Current Directions in Biomedical Engineering **3**(2), 371–374 (2017).
33. J. T. Russell, "Imaging Calcium Signals in Vivo: A Powerful Tool in Physiology and Pharmacology," Br. J. Pharmacol. **163**(8), 1605–1625 (2011).
34. O. Sirenko, M. K. Hancock, C. Crittenden, M. Hammer, S. Keating, C. B. Carlson, and G. Chandy, "Phenotypic assays for characterizing compound effects on induced pluripotent stem cell-derived cardiac spheroids," Assay Drug Dev. Technol. **15**(6), 280–296 (2017).
35. N. Huebsch, P. Loskill, M. A. Mandegar, N. C. Marks, A. S. Sheehan, Z. Ma, A. Mathur, T. N. Nguyen, J. C. Yoo, L. M. Judge, C. I. Spencer, A. C. Chukka, C. R. Russell, P. L. So, B. R. Conklin, and K. E. Healy, "Automated Video-Based Analysis of Contractility and Calcium Flux in Human-Induced Pluripotent Stem Cell-Derived Cardiomyocytes Cultured over Different Spatial Scales," Tissue Eng., Part C **21**(5), 467–479 (2015).